Research Paper

PD-L1^{ATTAC} mice reveal the potential of depleting PD-L1 expressing cells in cancer therapy

Elena Fueyo-Marcos[1], Gema Lopez-Pernas[1], Coral Fustero-Torre[2], Marta Elena Antón[1], Fátima Al-Shahrour[2], Oscar Fernández-Capetillo[1,3], Matilde Murga[1]

[1]Genomic Instability Group, Spanish National Cancer Research Centre (CNIO), Madrid 28029, Spain
[2]Bioinformatics Unit, Spanish National Cancer Research Centre (CNIO), Madrid 28029, Spain
[3]Department of Medical Biochemistry and Biophysics, Science for Life Laboratory, Division of Genome Biology, Karolinska Institute, S-171 21 Stockholm, Sweden

Correspondence to: Matilde Murga, Oscar Fernández-Capetillo; **email:** mmurga@cnio.es, ofernandez@cnio.es
Keywords: PD-L1, mouse models, inflammation, cancer, immunology
Received: January 14, 2023 **Accepted:** February 27, 2023 **Published:** March 22, 2023

ABSTRACT

Antibodies targeting the PD-1 receptor and its ligand PD-L1 have shown impressive responses in some tumors of bad prognosis. We hypothesized that, since immunosuppressive cells might present several immune checkpoints on their surface, the selective elimination of PD-L1 expressing cells could be efficacious in enabling the activation of antitumoral immune responses. To address this question, we developed an inducible suicidal knock-in mouse allele of *Pd-l1* (PD-L1^{ATTAC}) which allows for the tracking and specific elimination of PD-L1-expressing cells in adult tissues. Consistent with our hypothesis, elimination of PD-L1 expressing cells from the mouse peritoneum increased the septic response to lipopolysaccharide (LPS), due to an exacerbated inflammatory response to the endotoxin. In addition, mice depleted of PD-L1^{+} cells were resistant to colon cancer peritoneal allografts, which was associated with a loss of immunosuppressive B cells and macrophages, concomitant with an increase in activated cytotoxic CD8 T cells. Collectively, these results illustrate the usefulness of PD-L1^{ATTAC} mice for research in immunotherapy and provide genetic support to the concept of targeting PD-L1 expressing cells in cancer.

INTRODUCTION

Activation of T-cells involves binding of the T cell receptor (TCR) on T cells to peptide-bound major histocompatibility complexes (MHC) on antigen presenting cells (APCs). This activating signal is modulated by membrane-bound co-stimulatory receptors that potentiate the response or by co-inhibitory receptors which limit self-damage [1]. The discovery of immune checkpoint mediated by PD-1 and CTLA-4 receptors, and that targeting these pathways potentiates the antitumoral capabilities of our immune system led to the Nobel Prize in Medicine in 2018 [2]. Among all cancer immunotherapy strategies, antibodies targeting the PD-1/PD-L1 interaction have been the most intensively evaluated in clinical trials and are currently approved for a wide range of malignancies including melanoma, non-small cell lung cancer, Hodgkin´s lymphoma, head and neck squamous cell carcinoma or solid tumors presenting microsatellite instability (MSI) [3, 4]. Despite the undisputable success of this therapies, unfortunately only 20–40% of the patients respond to the therapy and even fewer show long-term responses [5, 6]. In addition, resistance to therapy, intrinsic or acquired, is also a frequent clinical finding in patients treated with immune checkpoint inhibitors (ICIs) [7]. Consistently, current efforts are directed to identify strategies that increase the percentage of patients that respond to cancer immunotherapy, and the efficacy of these treatments.

We hypothesized that, since PD-L1 expressing APCs might display additional immune checkpoint mediators on their membranes, their elimination could also exert antitumoral potential. In fact, recent studies have reported that chimeric antigenic receptor T (CAR-T) cells targeting PD-L1 reduce the growth of solid tumor xenografts in mice [8, 9]. To provide genetic proof-of-principle support for the validity of this approach, we generated mice carrying an inducible suicidal reporter allele of PD-L1. Besides its usefulness to identify and isolate PD-L1 expressing cells (PD-L1^{+}, hereafter) from adult mouse tissues, our work with these mice reveals that the selective elimination of PD-L1^{+} cells potentiates immune responses against different stimuli such as bacterial endotoxins or immunogenic cancer cells.

RESULTS AND DISCUSSION

Generation of an inducible suicidal mouse model of PD-L1

To generate an inducible suicidal reporter allele of PD-L1, we used the previously developed ATTAC (apoptosis through targeted activation of caspase 8) strategy [10]. In brief, we knocked in EGFP at the start codon of the mouse PD-L1 gene (*Cd274*), followed by FLAG-tagged catalytic domains of human caspase 8 fused to dimerizing serial FKBP domains which expression is driven by an IRES (Figure 1A). This *PD-L1^{ATTAC}* allele allows for the identification of PD-L1^{+} cells on the basis of EGFP expression, as well as their

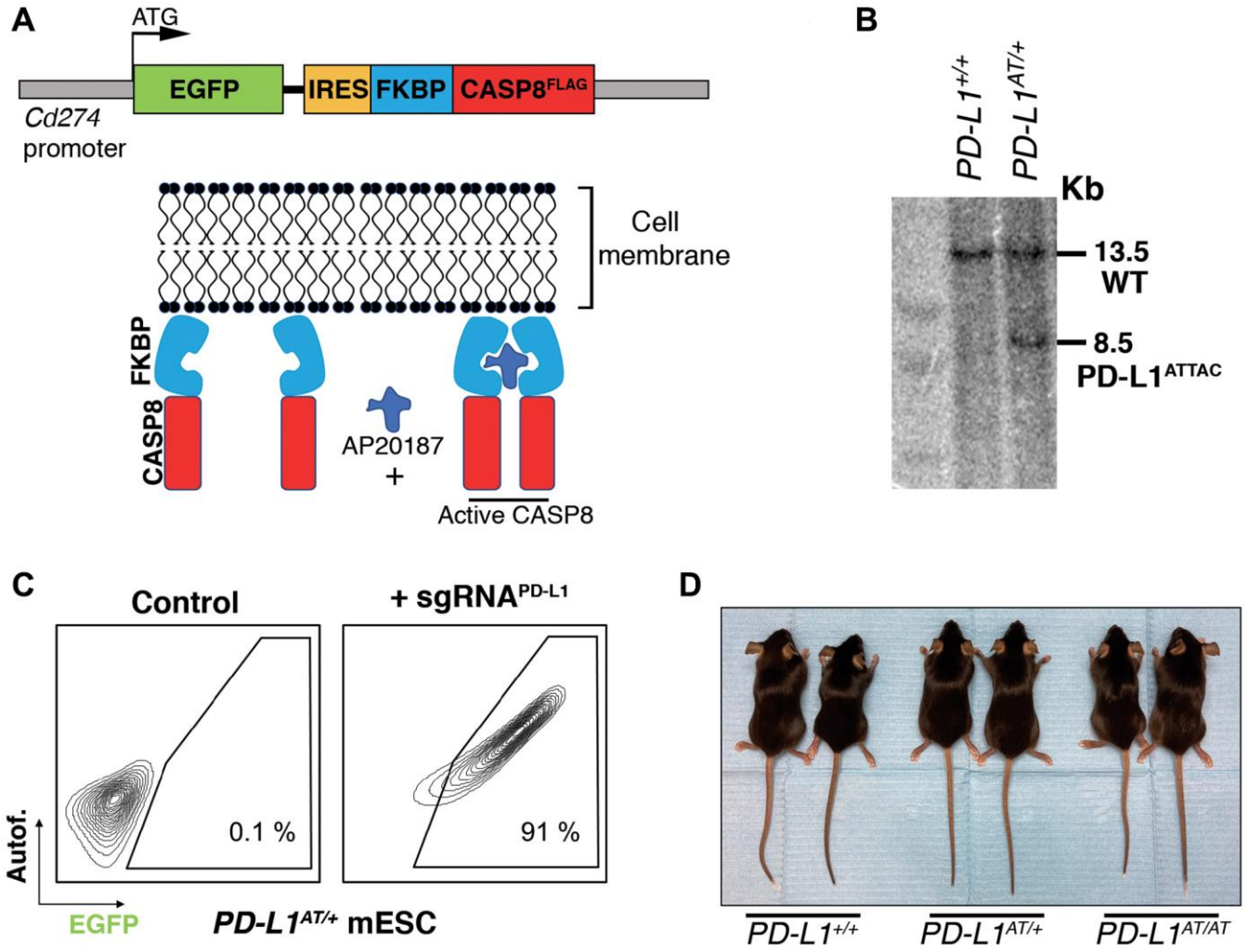

Figure 1. Generation of an inducible suicidal mouse model of PD-L1 (PD- L1^{ATTAC}). (**A**) Scheme illustrating the construct used for the generation of PD-L1^{ATTAC} mice. The construct is under control of *Cd274* promoter and codes for EGFP as a reporter gene and a FLAG-tagged caspase 8 fused to FKBP domains, which homodimerize in the presence of AP20187 and induce apoptosis of PD-L1^{+} cells. (**B**) Southern blot illustrating the presence of mESC clones harboring the correct integration of the PD-L1^{ATTAC} allele that were subsequently used for the generation of mutant mice. The 13.2 Kb band corresponds to the endogenous WT *Cd274* gene, and the 8.5 Kb band to the knock-in PD-L1^{ATTAC} allele. (**C**) FACS analyses of PD-L1 expression as monitored by EGFP in PD-L1^{ATTAC} mESC cells harboring a dead Cas9 compatible with the SAM CRISPR activator system and transduced or not with a sgRNA against the *Cd274* promoter. Percentage of EGFP+ cells is shown. (**D**) Representative picture from pairs of 3-month-old animals of the indicated genotypes.

selective killing through apoptosis upon treatment with the FK102 analogue AP20187. After identifying successfully recombined mouse embryonic stem cell (mESC) clones by Southern Blotting (Figure 1B) and before proceeding into generating mice, we first wanted to further confirm the correct integration of the allele by evaluating EGFP expression. To do so, we used the synergistic activation mediator (SAM) strategy, which enables CRISPR-dependent transcriptional activation of a selected gene [11]. Upon lentiviral transduction of *PD-L1*^{ATTAC} heterozygous mESC (*PD-L1*$^{AT/+}$) with an sgRNA targeting the *Cd274* promoter, EGFP expression was detected throughout the infected population (Figure 1C). *PD-L1*$^{AT/+}$ mESC were then used to generate mice using standard procedures and crosses between *PD-L1*^{ATTAC} heterozygous mice yielded *PD-L1*$^{+/+}$, *PD-L1*$^{AT/+}$ *and PD-L1*$^{AT/AT}$ animals at Mendelian rations. Mutant mice showed no apparent phenotype when compared to wild type (wt) littermates (Figure 1D). However, and consistent with the fact that *PD-L1*$^{AT/AT}$ animals are knockouts for *Pdl1*, allografts of B16-F10 melanoma cells presented more immune infiltrates and grew less when implanted in *PD-L1*$^{AT/AT}$ mice (Supplementary Figure 1).

In vitro validation of the PD-L1^{ATTAC} model

To evaluate the usefulness of the system *in vitro* we first generated mouse embryonic fibroblasts (MEF). Western Blotting (WB) revealed that a treatment with interferon gamma (IFNγ), a known inducer of PD-L1 expression [12, 13], triggered expression of EGFP in *PD-L1*$^{AT/+}$ and *PD-L1*$^{AT/AT}$ but not in wt MEF (Figure 2A). Conversely, PD-L1 expression was detectable in wt and *PD-L1*$^{AT/+}$ MEF but not in homozygous mutants, which is expected as the construct was inserted at the start codon and is thus a knockout allele (Figure 2A). Equivalent findings were made by immunofluorescence (IF) (Figure 2B) or flow cytometry (Figure 2C). Moreover, analysis of flow cytometry data revealed a full correlation between EGFP and PD-L1 expression in IFNγ-treated MEF (Figure 2D). In what regards to the cell killing induced by AP20187 and, to our surprise, we could only detect a significant impact in cell death if *PD-L1*$^{AT/+}$ or *PD-L1*$^{AT/AT}$ MEF were previously treated with IFNγ to trigger PD-L1 expression and also grown in low serum media (0.1% FBS) (Figure 2E). In contrast, AP20187 failed to significantly induce cell death if MEF were grown in media containing 10% FBS (Figure 2E). We hypothesized that this could be due to the ATTAC system being particularly efficient in killing non-growing cells as these cells might have a lower threshold for triggering apoptosis. In support of this view, we want to note that despite the usefulness of this strategy it has only been previously used to target non-dividing cells such as adipocytes, pancreatic islet beta cells or senescent cells [10, 14, 15].

Next, and given that immune cells are the main source of PD-L1 *in vivo*, we isolated splenocytes from adult mice, stimulated B cells with LPS and treated the cultures with IFNγ to induce PD-L1 expression. These experiments revealed a clear population of EGFP positive B cells (identified on the basis of B220 expression), which was selectively killed upon treatment with AP20187 (Figure 2F). Moreover, this cell killing could be prevented with a pan-caspase inhibitor, confirming that cell death was due to apoptosis (Figure 2F). Collectively, these data indicate that the *PD-L1*^{ATTAC} allele is efficient for the tracing of PD-L1^{+} cells, as well as for enabling their clearance in several cell types such as LPS-stimulated B cells or MEF.

In vivo validation of the PD-L1^{ATTAC} model

To evaluate the usefulness of the *PD-L1*^{ATTAC} allele as a reporter of PD-L1 expression *in vivo*, we first stained tissues of adult mice with an anti-EGFP antibody. As expected, EGFP expression was highest in organs from the immune system such as the spleen, lymph nodes, bone marrow or the thymus. In addition, scattered expression could also be detected in other organs such as the intestine, lungs or liver, while no expression was seen in the kidneys, pancreas, or hearts (Figure 3A and Supplementary Figure 2A). Similar observations were also made by WB (Figure 3B). Importantly, dual staining in lungs from wt and *PD-L1*$^{AT/+}$ animals identified that cells with cytoplasmic EGFP expression also presented PD-L1 on their membranes (Figure 3C), further supporting the reporter nature of the introduced mutation. Furthermore, while EGFP expressing cells were readily seen in homozygous *PD-L1*$^{AT/AT}$ lungs, these cells lacked PD-L1 expression, consistent with the null nature of the allele (Figure 3C). Immuno-fluorescence experiments further identified cells expressing both PD-L1 and EGFP in lungs from *PD-L1*$^{AT/+}$ mice (Figure 3D).

In what regards to the inducible-suicidal properties, we first evaluated the effects of an intraperitoneal (i.p.) administration of AP20187 in *PD-L1*^{ATTAC} mice. The treatment was particularly efficacious in killing EGFP+ cells in the peritoneum, although we also saw a significant effect in the lungs (Figure 3E). In contrast, this approach had no significant impact in reducing the percentage of EGFP expressing cells in the blood, thymus, spleen or lymph nodes (Figure 3E). FACS analyses confirmed a very efficient depletion of EGFP expressing cells from the peritoneum of *PD-L1*$^{AT/+}$ and *PD-L1*$^{AT/AT}$ mice after treatment with AP20187 (Figure 3F). We also evaluated if an intravenous (i.v.) administration of the drug could have more widespread effects. However, while i.v. delivery of AP20187 led to

a significant depletion of EGFP+ cells in the blood and bone marrow, we failed to see significant effects on other tissues (Supplementary Figure 2B). On the basis of these results, we decided to focus in the adult peritoneum as a model where to study the impact of selectively targeting PD-L1^{+} cells.

Depletion of PD-L1 expressing cells sensitizes mice to LPS

Intraperitoneal injection of the bacterial lipopolysaccharide (LPS) is a widely used experimental model of a lethal septic shock associated to a cytokine

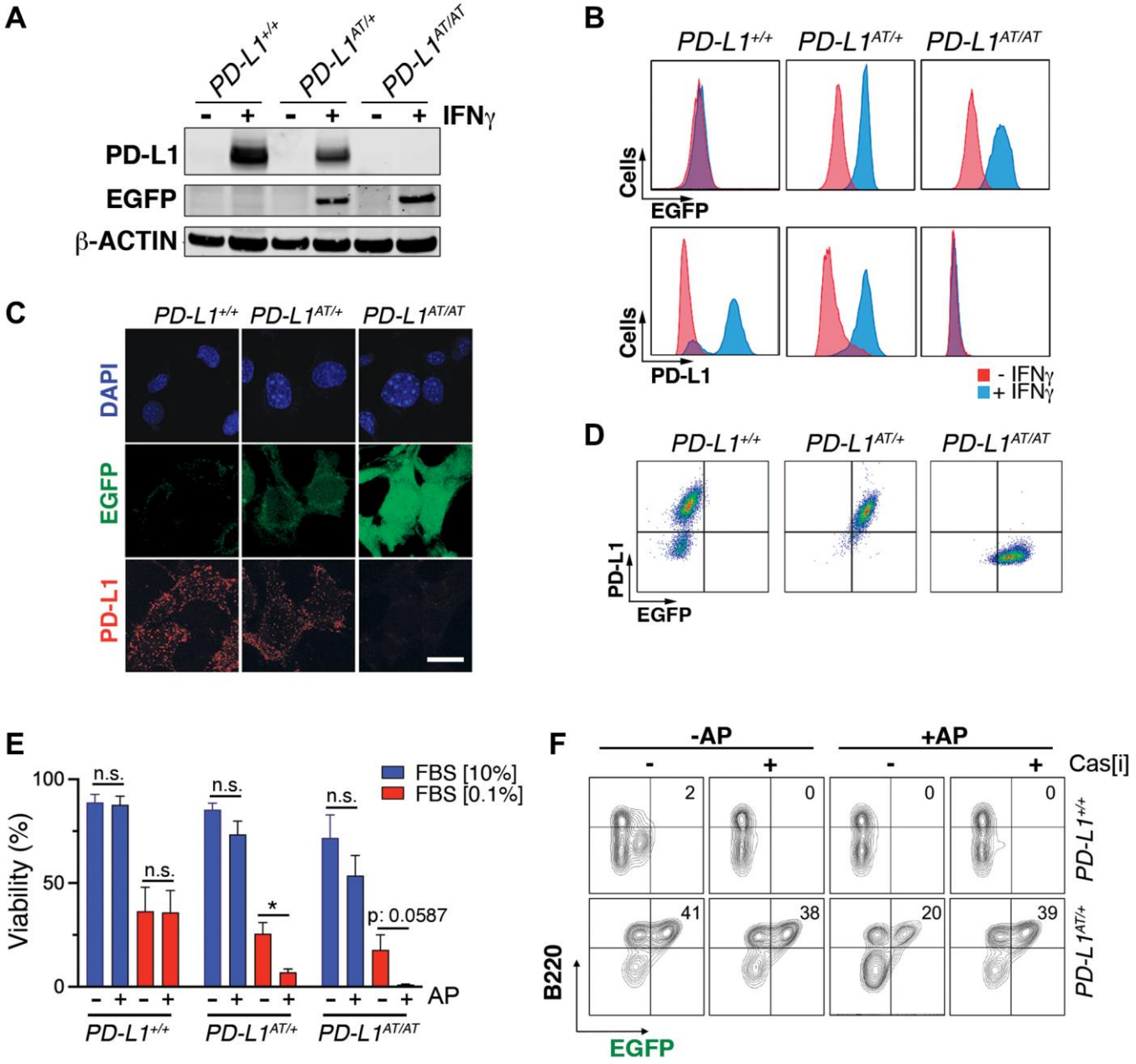

Figure 2. *In vitro* validation of the PD-L1^{ATTAC} mouse model. (**A**) Western blot illustrating PD-L1 and EGFP expression in *PD-L1*$^{+/+}$, *PD-L1*$^{AT/+}$ and *PD-L1*$^{AT/AT}$ MEFs exposed or not to IFNγ (100 ng/ml) for 48 hours. (**B**, **C**) Flow cytometry (**B**) and immunofluorescence (**C**) analyses of EGFP and PD-L1 expression in *PD-L1*$^{+/+}$, *PD-L1*$^{AT/+}$ and *PD-L1*$^{AT/AT}$ MEFs exposed to IFNγ (100 ng/ml) for 48 hours. Scale bar (white) indicates 5 µm. (**D**) Two-dimensional dot plot from the flow cytometry data shown in (**C**) illustrating the correlation between EGFP and PD-L1 expression per cell. (**E**) Percentage of live cells by FACS in *PD-L1*$^{+/+}$, *PD-L1*$^{AT/+}$ and *PD-L1*$^{AT/AT}$ MEFs cultured in normal or low-serum media (0.1% FBS) containing IFNγ (10 ng/ml) and treated or not with AP20187 (100 nM). Cells were cultured in normal or low-serum media for 24 hours. The day after, cells were exposed or not to AP20187 for 72 hours. (**F**) FACS analyses of B220 and EGFP expression of splenocytes from *PD-L1*$^{+/+}$ and *PD-L1*$^{AT/+}$ mice cultured in IFNγ (10 ng/ml), LPS (10 ng/ml) and M-CSF (10 ng/ml) for 24 hours before exposition to AP20187 (100 nM) and caspase inhibitor I (20 µM) for 24 hours. Percentage of B220+ EGFP+ cells is shown.

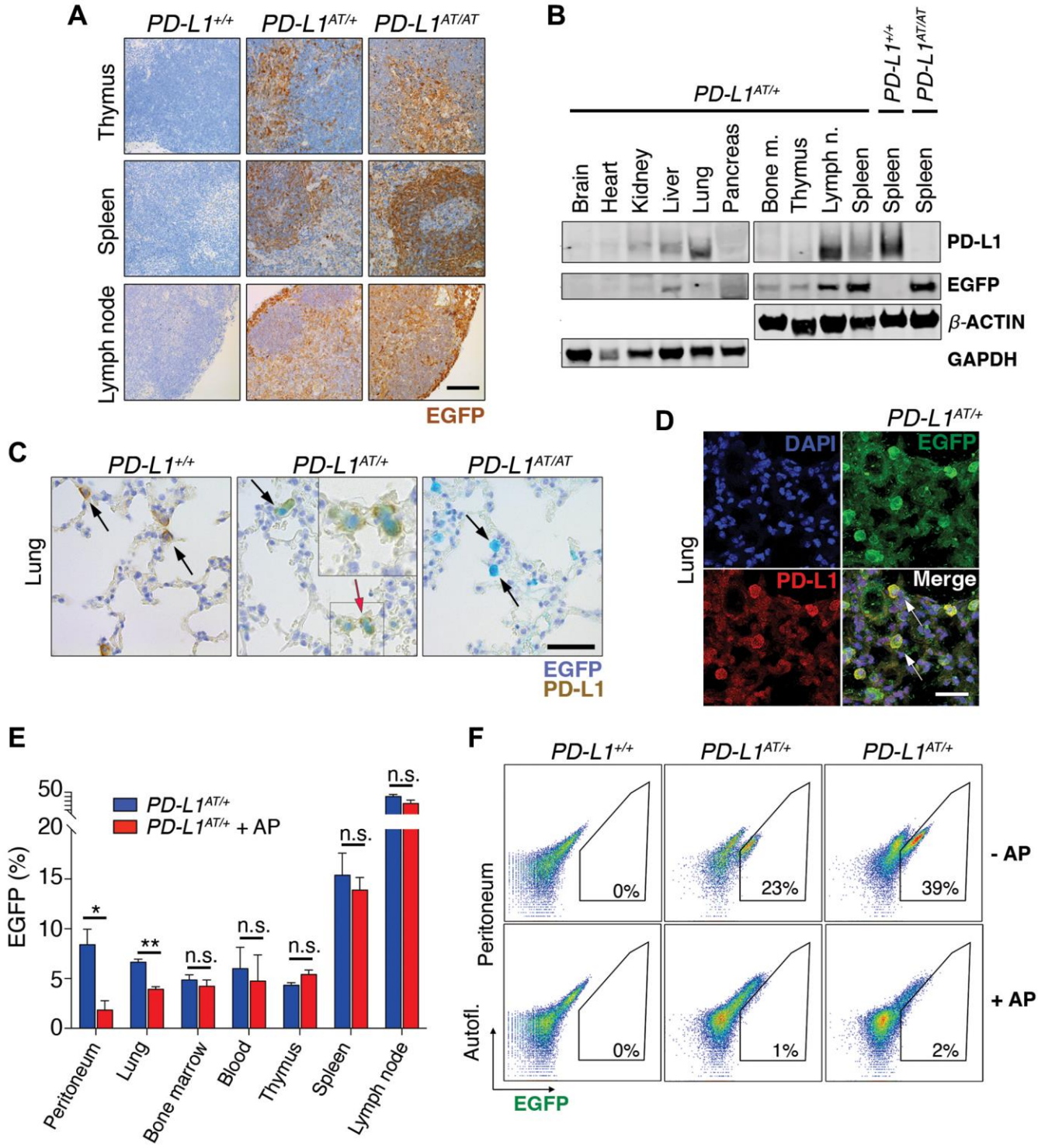

Figure 3. *In vivo* validation of the PD-L1^{ATTAC} mouse model. (**A**) EGFP immunohistochemistry (IHC) from the thymus, spleen and lymph nodes of *PD-L1*$^{+/+}$, *PD-L1*$^{AT/+}$ and *PD-L1*$^{AT/AT}$ mice. Scale bar (black) indicates 100 µm. (**B**) Western blot illustrating PD-L1 and EGFP expression in different organs of *PD-L1*$^{AT/+}$ mice and the spleen of wt and *PD-L1*$^{AT/AT}$ mice. Actin and GAPDH were used as a loading control. (**C**) Representative images from a dual PD-L1 and EGFP IHC in lungs from *PD-L1*$^{+/+}$, *PD-L1*$^{AT/+}$ and *PD-L1*$^{AT/AT}$ mice. Arrows indicate examples EGFP expressing cells. The red arrow in the *PD-L1*$^{AT/+}$ panel indicates an inset that is magnified in the right-hand corner to illustrate the appearance of cells expressing both EGFP and PD-L1. Scale bar (black) indicates 50 µm. (**D**) Representative image from a dual EGFP and PD-L1 IF in the lung of *PD-L1*$^{AT/+}$. Scale bar (white) indicates 30 µM. (**E**) Percentage of EGFP+ cells as revealed by FACS in different organs from control and AP20187 -treated (AP) *PD-L1*$^{AT/+}$ mice. AP20187 was administered via I.P. at 2.5 mg/kg for 3 days. The *p* value was calculated with unpaired *t*-test. Abbreviation: n.s.: non-significant; $^{*}p < 0.05$. $^{*}p < 0.01$ (**F**) FACS analysis of PD-L1 expression as monitored by EGFP in peritoneal cells from *PD-L1*$^{+/+}$, *PD-L1*$^{AT/+}$ and *PD-L1*$^{AT/AT}$ mice treated or not with AP20187 (2.5 mg/kg) for 3 days. Percentage of EGFP+ cells is shown.

storm [16]. Strikingly, while i.p. injections of AP20187 for three days did not affect LPS-mortality in wild type mice, it led to a significant reduction of the survival of *PD-L1*$^{AT/+}$ animals (Figure 4A, 4B). This effect was even more pronounced in *PD-L1*$^{AT/AT}$ mice with all animals dying by 18 hrs after LPS injection (with no wt animals being dead at this timepoint) (Figure 4C). Consistent with survival data, treatment of *PD-L1*$^{AT/+}$ and *PD-L1*$^{AT/AT}$ mice with AP20187 triggered a higher accumulation of the inflammatory cytokine IL-6 in the plasma of LPS-injected mice, confirming the increased severity of the septic shock (Supplementary Figure 3A–3C). Moreover,

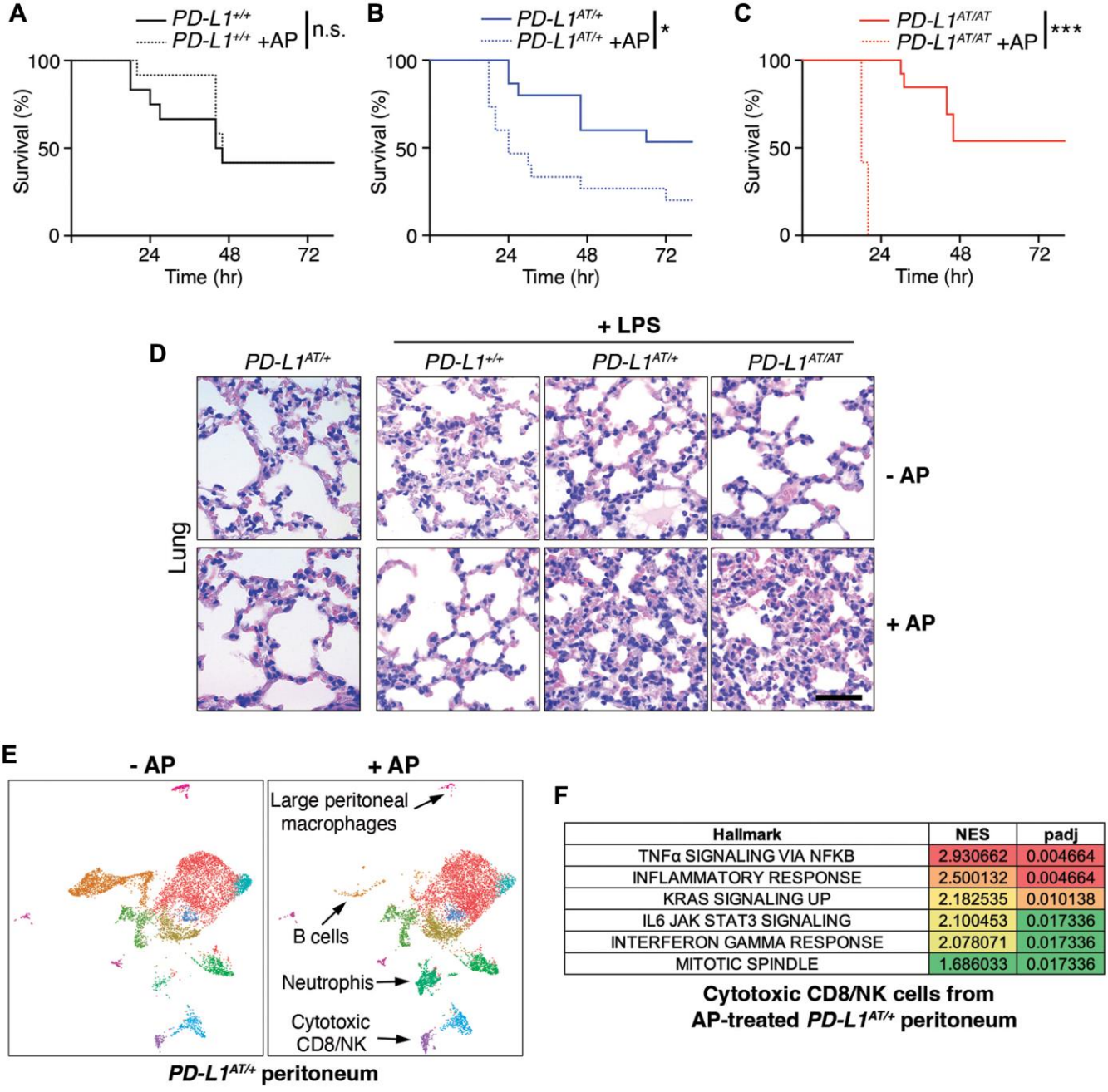

Hallmark	NES	padj
TNFα SIGNALING VIA NFKB	2.930662	0.004664
INFLAMMATORY RESPONSE	2.500132	0.004664
KRAS SIGNALING UP	2.182535	0.010138
IL6 JAK STAT3 SIGNALING	2.100453	0.017336
INTERFERON GAMMA RESPONSE	2.078071	0.017336
MITOTIC SPINDLE	1.686033	0.017336

Figure 4. Effects of depleting PD-L1-expressing cells in a model of LPS-induced septicaemia. (**A**–**C**) Kaplan-Meier survival curves of *PD-L1*$^{+/+}$, *PD-L1*$^{AT/+}$ and *PD-L1*$^{AT/AT}$ mice after LPS injection. Mice were treated via i.p. with AP20187 (2.5 mg/kg) for 3 days and subsequently injected i.p. with 10 mg/kg LPS. The *p* value was calculated with the Mantel-Cox log rank test. $^{*}p < 0.05$ $^{***}p < 0.001$. (**D**) Hematoxylin/eosin IHC in the lungs from the experiment defined in (**A**–**C**). Note the further accumulation of infiltrates in the lungs of AP20187-treated *PD-L1*$^{AT/+}$ and *PD-L1*$^{AT/AT}$ mice after LPS injection. Scale bar (black) indicates 75 µm. (**E**) Single-cell sequencing analysis of the impact of AP20187 treatment (2.5 mg/kg, 3 days) on the repertoire of peritoneal cells from *PD-L1*$^{AT/+}$ mice. Panels show UMAP plots from these analyses are shown and the cell types showing alterations are indicated by arrows. (**F**) GSEA analysis showing the hallmarks that were most significantly upregulated in cluster 9 (cytotoxic CD8/NK cells) after AP20187 treatment from the experiment defined in (**E**).

immunohistochemistry (IHC) analyses revealed a clear accumulation of immune infiltrates in the lungs or livers from AP20187-treated *PD-L1*$^{AT/+}$ and *PD-L1*$^{AT/AT}$ mice exposed to LPS (Figure 4D and Supplementary Figure 3D). Together, these data illustrate that the selective elimination of PD-L1^{+} cells increases the severity of immune responses in the mouse peritoneum.

To determine which changes in cell types were responsible for the observed effects, we conducted single cell RNA sequencing analyses of intraperitoneal cells from untreated or AP20187-treated *PD-L1*$^{AT/+}$ mice. These analyses revealed a drug-induced depletion of B cells and macrophages, concomitant to an accumulation of neutrophils and cytotoxic CD8/NK cells (Figure 4E and Supplementary Figure 3E). Moreover, Gene Set Enrichment Analyses (GSEA) indicate that CD8 cells from AP20187-treated *PD-L1*$^{AT/+}$ mice were hyperactivated, as revealed by the significant activation of several pathways such as those related to TNFα, IFNγ or IL-6 signaling, as well as a general activation of the inflammatory response (Figure 4F and Supplementary Figure 3F, 3G). Hence, depletion of PD-L1^{+} cells alters the intraperitoneal immune repertoire which includes the accumulation of activated cytotoxic CD8 cells.

Depletion of PD-L1^{+} cells increases survival to peritoneal tumor allografts

Finally, and given that cytotoxic T cells are thought to be the main effectors in the context of anti-PD-L1 immunotherapies [17], we tested the impact of depleting PD-L1^{+} cells in of cancer. To this end, we used a model of intraperitoneal metastasis by the highly immunogenic colon adenocarcinoma cell line MC-38, which can be used for allografts in immuno-competent mice and is sensitive to anti-PD-L1 therapies [18]. Furthermore, dissemination of cancer cells into the peritoneum is frequent in digestive and gynecological cancers and is associated with poor prognosis [19], highlighting the relevance of the chosen model.

To conduct these experiments, we first generated a MC-38 clone harboring constitutive expression of firefly luciferase which enables monitoring tumor progression by intravital imaging (MC-38^{luc}). Intraperitoneal injection of MC-38^{luc} cells led to a lethal disease associated to the dissemination and growth of cancer cells in the peritoneal cavity (Figure 5A). Treatment with AP20187 did not affect the progression of the disease in wt mice (Supplementary Figure 4A).

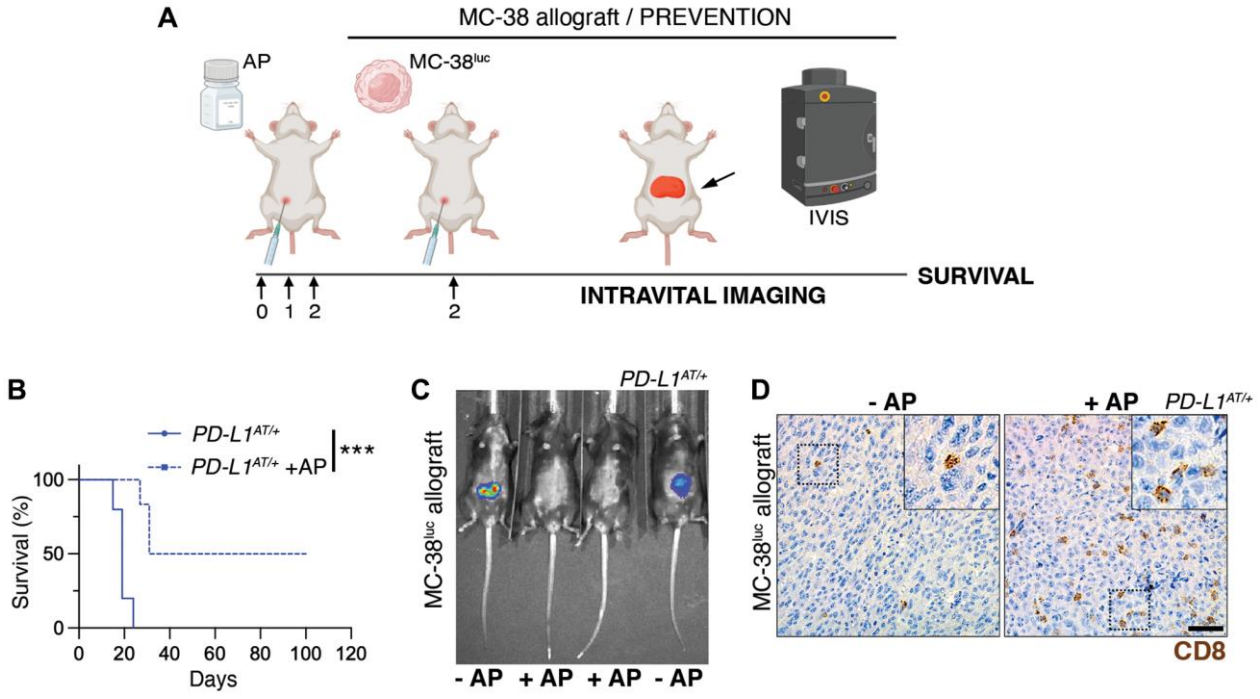

Figure 5. Depleting PD-L1^{+} cells prolongs survival in an immunocompetent model of peritoneal cancer metastasis. (**A**) Schematic overview of the prevention experimental workflow. 5 × 10^{5} MC-38^{luc} cells were intraperitoneally injected into mice that were previously injected i.p. for 3 consecutive days with AP20187 (2.5 mg/kg). (**B**) Kaplan-Meier survival curve of control and AP20187-pretreated *PD-L1*$^{AT/+}$ mice after i.p. inoculation of MC-38^{luc} allografts. The *p* value was calculated with the Mantel-Cox log rank test. ***$p <$ 0.001. (**C**) Representative IVIS image of mice from the experiment defined in (**B**) at day 4 post-tumor injection. (**D**) IHC of CD8 in intraperitoneal MC-38^{luc} allografts isolated from control and AP20187-treated *PD-L1*$^{AT/+}$ mice. Insets in each panel are magnified to illustrate the presence of tumor-infiltrating CD8^{+} cells. Scale bar (black) indicates 30 µm.

Strikingly, while all *PD-L1*$^{AT/+}$ mice were dead within the first month after being intraperitoneally injected with MC-38^{luc} cells, a prior treatment with AP20187 prior to the injection of MC-38 cells led to survival of half of the animals (Figure 5B). Consistently, intravital imaging showed a clear reduction of MC-38 cells in the peritoneum of AP20187-treated *PD-L1*$^{AT/+}$ mice (Figure 5C). Furthermore, and similar to our previous observations in the LPS-sepsis model, intraperitoneal tumors from AP20187-treated presented a significant accumulation of infiltrating CD8 lymphocytes, highlighting the increased immune response to the tumor (Figure 5D). Besides this prevention model, AP20187 treatment also increased the survival of *PD-L1*$^{AT/+}$ mice if the drug was administered 4 days after the injection of MC-38 cells (treatment model) (Supplementary Figure 4B–4D). Together with the data from the LPS-induced septic shock, these experiments indicate that the selective targeting of PD-L1^{+} cells intensifies immune responses in the peritoneum, which in the context of cancer is protective and favours the clearance of tumor cells.

In summary, we here present PD-L1^{ATTAC} as a reporter and inducible suicidal allele of mouse PD-L1. The reporter EGFP enables the identification and isolation of PD-L1^{+} cells from adult tissues, which we believe is useful as antibodies detecting mouse PD-L1 often give signal in PD-L1 deficient samples. As for the inducible-suicidal strategy, our experiments indicate that this effect is significantly influenced by the administration route for AP20187 and growth rates of the cells, which we wonder to what extent could also have influenced previous studies using the ATTAC strategy. Despite these limitations, i.p. administration of AP20187 yields a very efficient depletion of PD-L1^{+} from the peritoneum, enabling functional studies to investigate the impact of depleting PD-L1^{+} cells *in vivo*. Of note, no significant toxicities were observed in mice that were i.p. treated for up to 3 months with 3 weekly doses of AP20187. Our results confirm that the selective elimination boosts immune responses in the peritoneum, which prolongs survival against a model of peritoneal cancer metastasis. Hence, our work supports the usefulness of targeting PD-L1 expressing cells in cancer therapy, and provides the immunotherapy research community with a useful genetic tool for investigations on the PD-1/PD-L1 checkpoint in mice.

MATERIALS AND METHODS

Mouse models

The PD-L1^{ATTAC} targeting vector was generated by recombineering (Genebridges, Germany). Recombinant ES cells were screened by Southern Blot through standard procedures, and subsequently used for the generation of chimaeras by aggregation. Animals were genotyped by PCR using the following primers (UP: 5′-TTGCTTCAGTTACAGCTGGCTCG-3′; Down_WT: 5′-CGTAGCAAGTGACAGCAGGCTG-3′; Down_MUT: 5′-GCCGTTTACGTCGCCGTCCAG-3′). Mice were kept under standard conditions at specific-pathogen free facility of the Spanish National Cancer Centre in a mixed C57BL/6-129/Sv background. 9–12-week-old mice were used for all experiments. All mouse work was performed in accordance with the Guidelines for Humane Endpoints for Animals Used in Biomedical Research, and under the supervision of the Ethics Committee for Animal Research of the "Instituto de Salud Carlos III".

AP20187 treatments

AP20187 (MedChemExpress, HY-13992) was resuspended in 75% EtOH at 62.5 mg/ml and stored at −20°C. For *in vitro* experiments, cells were treated with 100 nM AP20187 for 48–72 h. *In vivo*, the compound was dissolved in 2% Tween-20 (Sigma-Aldrich, P7949) and 10% PEG-300 (Sigma-Aldrich #202371) and mice were i.p. injected with 2.5 mg/kg AP20187.

LPS-induced septicemia

Mice were injected i.p. with AP20817 (2.5 mg/kg) for 3 consecutive days before an i.p. injection of LPS (10 mg/kg, Sigma-Aldrich, #L2630) resuspended in PBS. Blood, plasma and tissues were isolated for further IHC and ELISA analyses. Mice were monitored for overall health and for a week after LPS injection.

MC-38^{luc} allografts

Mice were injected i.p. with 5 × 10^{5} MC-38^{luc} cells. Tumor growth was monitored twice a week by intravital imaging using an IVIS Optica Imaging system (Perkin Elmer) after anesthetizing mice with Isoflurane. For IVIS analyses, animals were previously injected i.p. with 150 mg/kg D-Luciferin (Xenolight, #122799).

Statistics

All statistical analyses were performed using Prism software (GraphPad Software) and statistical significance was determined where the *p*-value was <0.05 (*), <0.01 (**), <0.001 (***) and <0.0001 (****). Survival data was evaluated using Kaplan-Meier analyses.

Extended Methods for this manuscript can be found in the Supplementary Materials.

AUTHOR CONTRIBUTIONS

E.F. contributed to most of the experiments; C.F. and F.A.-S. helped with bioinformatic analyses of scRNAseq data; G.L.-P. helped with *in vivo* experiments and IHC analyses; M.A. provided technical help; O.F. helped to supervise the work and to write the manuscript; M.M. coordinated the study, contributed to experiments and helped with manuscript writing.

CONFLICTS OF INTEREST

The authors declare no conflicts of interest related to this study.

ETHICAL STATEMENT

Mice were maintained in a mixed C57BL/6-Sv background under standard housing conditions with free access to chow diet and water, as recommended by the Federation of European Laboratory Animal Science Association. All mice work was performed in accordance with the Guidelines for Humane Endpoints for Animals Used in Biomedical Research, and under the supervision of the Ethics Committee for Animal Research of the "Instituto de Salud Carlos III", following the procedures detailed in the approved ethics protocol (PROEX 264/19).

FUNDING

O.F-C. is supported by grants from the Spanish Ministry of Science, Innovation and Universities (PID2021-128722OB-I00, co-financed with European FEDER funds) and the Spanish Association Against Cancer (AECC; PROYE20101FERN) to O.F-C. and by a Ph.D. fellowship from María Oliva-Amigos/as del CNIO to E.F-M. The CNIO Bioinformatics Unit (BU) is a member of the Spanish National Bioinformatics Institute (INB), ISCIII- Bioinformatics platform and is supported by grant PT17/0009/0011, of the Acción Estratégica en Salud 2013–2016 of the Programa Estatal de Investigación Orientada a los Retos de la Sociedad, funded by the ISCIII and European Regional Development Fund (ERDF-EU) and project RETOS RTI2018-097596-B-I00 funded by AEI-MCIU and cofounded by the ERDF-EU. The authors declare no competing financial interests.

REFERENCES

1. Smith-Garvin JE, Koretzky GA, Jordan MS. T cell activation. Annu Rev Immunol. 2009; 27:591–619. https://doi.org/10.1146/annurev.immunol.021908.132706 PMID:19132916

2. Kroemer G, Zitvogel L. Immune checkpoint inhibitors. J Exp Med. 2021; 218:e20201979. https://doi.org/10.1084/jem.20201979 PMID:33600556

3. Gong J, Chehrazi-Raffle A, Reddi S, Salgia R. Development of PD-1 and PD-L1 inhibitors as a form of cancer immunotherapy: a comprehensive review of registration trials and future considerations. J Immunother Cancer. 2018; 6:8. https://doi.org/10.1186/s40425-018-0316-z PMID:29357948

4. Sun C, Mezzadra R, Schumacher TN. Regulation and Function of the PD-L1 Checkpoint. Immunity. 2018; 48:434–52. https://doi.org/10.1016/j.immuni.2018.03.014 PMID:29562194

5. Garon EB, Hellmann MD, Rizvi NA, Carcereny E, Leighl NB, Ahn MJ, Eder JP, Balmanoukian AS, Aggarwal C, Horn L, Patnaik A, Gubens M, Ramalingam SS, et al. Five-Year Overall Survival for Patients With Advanced Non-Small-Cell Lung Cancer Treated With Pembrolizumab: Results From the Phase I KEYNOTE-001 Study. J Clin Oncol. 2019; 37:2518–27. https://doi.org/10.1200/JCO.19.00934 PMID:31154919

6. Hamid O, Robert C, Daud A, Hodi FS, Hwu WJ, Kefford R, Wolchok JD, Hersey P, Joseph R, Weber JS, Dronca R, Mitchell TC, Patnaik A, et al. Five-year survival outcomes for patients with advanced melanoma treated with pembrolizumab in KEYNOTE-001. Ann Oncol. 2019; 30:582–8. https://doi.org/10.1093/annonc/mdz011 PMID:30715153

7. Sharma P, Hu-Lieskovan S, Wargo JA, Ribas A. Primary, Adaptive, and Acquired Resistance to Cancer Immunotherapy. Cell. 2017; 168:707–23. https://doi.org/10.1016/j.cell.2017.01.017 PMID:28187290

8. Qin L, Zhao R, Chen D, Wei X, Wu Q, Long Y, Jiang Z, Li Y, Wu H, Zhang X, Wu Y, Cui S, Wei W, et al. Chimeric antigen receptor T cells targeting PD-L1 suppress tumor growth. Biomark Res. 2020; 8:19. https://doi.org/10.1186/s40364-020-00198-0 PMID:32514352

9. Xie YJ, Dougan M, Jailkhani N, Ingram J, Fang T, Kummer L, Momin N, Pishesha N, Rickelt S, Hynes RO, Ploegh H. Nanobody-based CAR T cells that target the tumor microenvironment inhibit the growth of solid tumors in immunocompetent mice. Proc Natl Acad Sci U S A. 2019; 116:7624–31. https://doi.org/10.1073/pnas.1817147116 PMID:30936321

10. Pajvani UB, Trujillo ME, Combs TP, Iyengar P, Jelicks L, Roth KA, Kitsis RN, Scherer PE. Fat apoptosis through targeted activation of caspase 8: a new mouse model of inducible and reversible lipoatrophy. Nat Med. 2005; 11:797–803. https://doi.org/10.1038/nm1262 PMID:15965483

11. Konermann S, Brigham MD, Trevino AE, Joung J, Abudayyeh OO, Barcena C, Hsu PD, Habib N, Gootenberg JS, Nishimasu H, Nureki O, Zhang F. Genome-scale transcriptional activation by an engineered CRISPR-Cas9 complex. Nature. 2015; 517:583–8. https://doi.org/10.1038/nature14136 PMID:25494202

12. Kim J, Myers AC, Chen L, Pardoll DM, Truong-Tran QA, Lane AP, McDyer JF, Fortuno L, Schleimer RP. Constitutive and inducible expression of b7 family of ligands by human airway epithelial cells. Am J Respir Cell Mol Biol. 2005; 33:280–9. https://doi.org/10.1165/rcmb.2004-0129OC PMID:15961727

13. Lee SK, Seo SH, Kim BS, Kim CD, Lee JH, Kang JS, Maeng PJ, Lim JS. IFN-gamma regulates the expression of B7-H1 in dermal fibroblast cells. J Dermatol Sci. 2005; 40:95–103. https://doi.org/10.1016/j.jdermsci.2005.06.008 PMID:16085391

14. Baker DJ, Wijshake T, Tchkonia T, LeBrasseur NK, Childs BG, van de Sluis B, Kirkland JL, van Deursen JM. Clearance of p16Ink4a-positive senescent cells delays ageing-associated disorders. Nature. 2011; 479:232–6. https://doi.org/10.1038/nature10600 PMID:22048312

15. Wang ZV, Mu J, Schraw TD, Gautron L, Elmquist JK, Zhang BB, Brownlee M, Scherer PE. PANIC-ATTAC: a mouse model for inducible and reversible beta-cell ablation. Diabetes. 2008; 57:2137–48. https://doi.org/10.2337/db07-1631 PMID:18469203

16. Redl H, Schlag G, Bahrami S. Animal models of sepsis and shock: a review and lessons learned. Edwin A Deitch. Shock 9(1):1-11, 1998. Shock. 1998; 10:442–5. PMID:9872685

17. Tumeh PC, Harview CL, Yearley JH, Shintaku IP, Taylor EJ, Robert L, Chmielowski B, Spasic M, Henry G, Ciobanu V, West AN, Carmona M, Kivork C, et al. PD-1 blockade induces responses by inhibiting adaptive immune resistance. Nature. 2014; 515:568–71. https://doi.org/10.1038/nature13954 PMID:25428505

18. Juneja VR, McGuire KA, Manguso RT, LaFleur MW, Collins N, Haining WN, Freeman GJ, Sharpe AH. PD-L1 on tumor cells is sufficient for immune evasion in immunogenic tumors and inhibits CD8 T cell cytotoxicity. J Exp Med. 2017; 214:895–904. https://doi.org/10.1084/jem.20160801 PMID:28302645

19. Mikuła-Pietrasik J, Uruski P, Tykarski A, Książek K. The peritoneal "soil" for a cancerous "seed": a comprehensive review of the pathogenesis of intraperitoneal cancer metastases. Cell Mol Life Sci. 2018; 75:509–25. https://doi.org/10.1007/s00018-017-2663-1 PMID:28956065

SUPPLEMENTARY MATERIALS

Extended Methods

Cell culture

293T cells (ATCC) were grown in DMEM supplemented with 10% FBS and 1% Penicillin/ Streptomycin and transfected in media containing no antibiotics. MC- 38 cells (kind gift from Eduard Batllé) were cultured in DMEM supplemented with 10% FBS and 1% Penicillin/Streptomycin. For the generation of an MC-38 clone expressing luciferase, MC-38 cells were transduced with "pLenti CMV B5-Luc Blast" lentiviruses (Addgene, #21474). MEFs isolated from 13.5 d.p.c. embryos were cultured in DMEM (Sigma, D5796) supplemented with 10%–15% FBS (Sigma) and 1% Penicillin/Streptomycin (Gibco, #11548876) in low-oxygen conditions. Cells were passaged every 3 or 4 days in a 1:4 ratio. IFNγ (Peprotech, #315–05) was added to culture media at 10, 50 or 100 ng/ml concentration. For the experiments assessing the effect of AP20187, MEFs were plated in DMEM containing 10% FBS for 2 days in the presence or absence of IFNγ (10 ng/ml). To evaluate the effect of the drug in non-growing cells, MEF were washed twice with PBS and grown in low-serum media (0.1% FBS) for 3 days in the presence or absence of IFNγ. In all cases, AP20187 was added to culture media at a final concentration of 100 nM for the last 3 days. Resting splenic B cells were isolated and cultured in IFNγ (10 ng/ml), LPS (10 ng/ml) (Sigma, L2630) and M-CSF (10 ng/ml) for 24 hours before exposition to AP20187 (100 nM) with or without the caspase inhibitor I (20 μM) (Sigma-Aldrich, #627610) for 24 hours.

Lentiviral infection

Lentiviruses were produced by transfection of 293T cells with lentiviral transfer vectors and the packaging plasmids pMDL, pRev and VsVg at a 1:0.65:0.25:0.35 ratio. Transfection was performed using Lipofectamine 2000 (ThermoFisher, #11668019) and Opti-MEM Reduced Serum Medium (Gibco, #31985070) as recommended by the manufacturer. Viral supernatants were collected 48 h following transfection, filtered through a 0.45 μm filter and either added to target cells or frozen at −80°C.

CRISPR activation

In order to obtain SAM-compatible mESC, PD-L1$^{AT/+}$ mESC were simultaneously infected with lentiviruses coding for MS2-p65-HSF1 and dCas9-VP64 [1]. Two days after infection, cells were selected with 10 μg/ml blasticidin (Invitrogen) and 200 μg/ml hygromycin B (Calbiochem). Selected clones were transduced with lentiviruses expressing a sgRNA targeting the *Cd274* promoter (5′-CACCGTTCGGTTTCACAGACA GCGG-3′) and EGFP expression was evaluated by flow cytometry.

Immunohistochemistry

Tissues were fixed in formalin and embedded in paraffin for subsequent processing. Consecutive 2.5-μm sections were treated with citrate for antigenic recovery and processed for immunohistochemistry with antibodies against EGFP (Cell signaling, #2956), mPD-L1 (Abcam, ab213480), CD8 (CNIO Monoclonal Antibody Unit, clone OTO94A) and CD45 (BD Biosciences, #553089). IHCs were scanned and digitalized with a MIRAX system (Zeiss) for further analyses.

Flow cytometry

Cells were trypsinized, pelleted and resuspended in PBS with DAPI. For experiments using AP20187, culture media and the PBS from the washing steps were also collected to include dead cells in the analyses. Cells were blocked with PBS +1% BSA (Roche #10735086001) for 30 minutes and stained with an anti- mPD-L1 antibody antibody (Biolegend, 124313). mPD-L1 and EGFP expression were then evaluated by flow cytometry with a FACSCanto II (BD Biosciences), and data analysed with FlowJo (BD Biosciences).

Immunoblotting

For WB analyses, cells were washed once with PBS, and lysed in RIPA buffer (Tris-HCl 50 mM, pH 7.4, NP-40 1%, Na-deoxycholate 0.25%, NaCl: 150 mM, EDTA 1 mM) containing protease and phosphatase inhibitors (Sigma-Aldrich). Samples were resolved by SDS-PAGE and analyzed by standard WB techniques. Primary antibodies against GFP, PD-L1, GAPDH and β-ACTIN were used (see the list at the end of the Methods section with the references to the antibodies). Protein blot analyses were performed on the LICOR platform (BD Biosciences).

In vitro immunofluorescence

MEFs were grown on a IbiTreat μSlide 8 well plate (Ibidi, #80826) and fixed with 1% PFA (EMS, #15710). Cells were blocked with PBS containing 1% BSA (Roche, #10735086001) for 30 minutes at RT and incubated with anti-mPD-L1 primary antibody (CNIO Monoclonal Antibody Unit, clone GOYA536A) in PBS for 1 hour at RT and Goat anti-Rat IgG (H+L) Alexa

Fluor 594 (Invitrogen, A11007) in PBS for 1 hour at RT. Nuclei were counterstained using 10 μg/ml Hoechst 33342 (Invitrogen, H3570) in 2× SSC for 30 minutes at RT. Images were acquired using a SP8 microscope (Leica) with a 63× magnification lens at non-saturating conditions. Images were then processed with ImageJ.

Tissue immunofluorescence

Immunofluorescence on tissue sections was carried out as previously described [2]. Briefly, after antigen retrieval, the sections are rinsed, and permeabilised in PBS containing 0.25% Triton X100 and 0.2% gelatine. After that, they were blocked in 5% BSA in permeabilisation buffer. Sections were then incubated with the primary antibodies in 1% BSA overnight at room temperature, and with the secondary antibodies for 1 h at room temperature. Finally, after rinsing, the sections are incubated in 10 mM CuSO4/50 mM NH4Cl solution, dried, and mounted with ProLong Gold antifade (ThemoFisher, P10144) mounting media. Images were captured with a Leica SP5 WLL confocal microscope. A 40× magnification lens was used and images were taken at non-saturating conditions.

Anti-mouse PD-L1 mAb

A new anti-mouse PD-L-1 mAb (clone GOYA536A) was produced by immunizing Wistar rats with HEK293-expressed extracellular domain (ec) of PD-L1 fused to Fc fragment. Wistar rats (Charles River Laboratories, France) were injected intraperitoneally (three times at 14-day intervals) with 100 μg of ecPDL1-Fc and Complete Freund's adjuvant (Difco). A 150 μg last booster of the recombinant ecPD-L1-Fc protein was injected intraperitoneally and splenocytes were isolated and fused 3 days later. Hybridoma supernatants were screened by ELISA using HEK293T cells transfected with the PCMV6-mPDL1-MYC-DDK plasmid (Origene, #MR203953). The rat mAb that was raised against mouse PD- L1 (clone GOYA536A) was cloned by the limiting dilution technique. All animal experiments were performed under the experimental protocol approved by the Institutional Committee for Care and Use of Animals from Consejería de Medio Ambiente y Ordenación del Territorio of the Comunidad de Madrid (Madrid, Spain) with reference number PROEX62.3/20. All efforts were made to minimizeanimal suffering.

ELISA

IL-6 levels were quantified by an anti mIL-6 ELISA kit (Invitrogen #88-7064-22) following manufacturer's instructions. Plates were analyzed using a Victor microplate reader (Perkin Elmer).

Droplet based single-cell mRNA sequencing

Peritoneal cavity cells were obtained by peritoneal lavage following standard procedures. Cells were collected in cold PBS containing 5% FBS and 1 mM EDTA to preserve cell viability. Cell suspension was washed with PBS containing BSA and filtered through a 40 μm cell strainer. Viable cells were enriched by magnetic separation using the Dead Cell Removal Kit (Miltenyi Biotec #130-090-101). Isolated cells were next washed and finally suspended in PBS-0.04% ultrapure BSA (Invitrogen #AM2616) at 1000 cells/μl, and shown to have a viability higher than 95% by Trypan Blue exclusion (Gibco #15250061). Approximately 10^4 cells from each sample were loaded onto a 10X Chromium Single Cell Controller chip B (10× Genomics) following manufacturer's instructions (Chromium Single Cell 3′ GEM, Library and Gel Bead Kit v3, PN-1000075). Generation of gel beads in emulsion (GEMs), barcoding, GEM-RT clean up, cDNA amplification and library construction were all performed according to manufacturer's recommendations. Libraries were sequenced in an asymmetrical pair-end format, with 28 bases for read 1 and 56 for read 2 in a NextSeq550 instrument (Illumina) with v2.5 reagentkits.

scRNAseq data analysis

Bcl files were converted to fastq format with cellranger mkfastq (10× Genomics), a wrapper for bcl2fastq (Illumina), and subsequently analysed with/by the bollito pipeline [3]. Reads were aligned to the Gencode mouse reference (GRCm38) and quantified using the STARsolo aligner [4]. The Seurat toolkit [5] was used to perform the cell-based quality control, normalisation, integration and clustering steps. We filtered out cells with less than 750 genes detected and high mitochondrial (>10%) and ribosomal (>40%) gene content. Cells with more than 4000 detected genes were considered doublets. Low- abundance genes, those expressed in less than 2 cells, were also removed from the dataset. A total of 14347 cells were recovered. Samples were normalised using the sctransform approach [6] and integrated. The first 20 components were selected to cluster the samples and a Uniform Manifold Approximation and Projection (UMAP) was applied for their visualisation. We used the SingleR [7] annotation scores to guide the annotation of each cluster. Differential gene expression was performed using Seurat's Wilcox test. Genes expressed in less than 25% of the cells were filtered out. The estimated significance level (*P* value) was corrected to account for multiple hypotheses testing using Benjamini and Hochberg False DiscoveryRate (FDR) adjustment. Genes with FDR less than or equal to 0.05 were selected as differentially expressed. Significantly upregulated or downregulated genes were introduced into PANTHER

to perform a Gene Ontology Biological Process enrichment analysis (http://geneontology.org) [8–10]. Finally, a Gene set enrichment analysis (GSEA) was performed using the fgsea package [11].

Antibodies

Antibody	Use	Dilution	References
GFP	WB	1:1000	Cell Signaling, #2956
PD-L1	WB	1:1000	Abcam, ab213480
GAPDH	WB	1:1000	Cell Signaling, #2118
β-ACTIN	WB	1:50000	Sigma, A5441
CD45R/B220 PE	FACS	1:400	BD Biosciences, 553089
PD-L1 PE-Cy7	FACS	1:400	Biolegend, 124313
GFP	IHC	1:100	Cell signaling, #2956
PD-L1	IHC	1:2000	Abcam, ab213480
CD45	IHC	1:200	Cell signaling, #557390
CD8a	IHC	1:200	Clone OTO94A*
PD-L1	Tissue IF	1:500	Abcam, ab213480
GFP	Tissue IF	1:500	Abcam, ab13970
mPD-L1	IF	1:20	Clone GOYA536A*

Supplementary References

1. Konermann S, Brigham MD, Trevino AE, Joung J, Abudayyeh OO, Barcena C, Hsu PD, Habib N, Gootenberg JS, Nishimasu H, Nureki O, Zhang F. Genome-scale transcriptional activation by an engineered CRISPR-Cas9 complex. Nature. 2015; 517:583–8. https://doi.org/10.1038/nature14136 PMID:25494202

2. Zaqout S, Becker LL, Kaindl AM. Immunofluorescence Staining of Paraffin Sections Step by Step. Front Neuroanat. 2020; 14:582218. https://doi.org/10.3389/fnana.2020.582218 PMID:33240048

3. García-Jimeno L, Fustero-Torre C, Jiménez-Santos MJ, Gómez-López G, Di Domenico T, Al-Shahrour F. bollito: a flexible pipeline for comprehensive single-cell RNA-seq analyses. Bioinformatics. 2022; 38:1155–6. https://doi.org/10.1093/bioinformatics/btab758 PMID:34788788

4. Bilbaum AJW, Dobin A. STARsolo: single-cell RNA-seq analyses beyond gene expression. F1000Res. 2019.

5. Stuart T, Butler A, Hoffman P, Hafemeister C, Papalexi E, Mauck WM 3rd, Hao Y, Stoeckius M, Smibert P, Satija R. Comprehensive Integration of Single-Cell Data. Cell. 2019; 177:1888–1902.e21. https://doi.org/10.1016/j.cell.2019.05.031 PMID:31178118

6. Hafemeister C, Satija R. Normalization and variance stabilization of single-cell RNA-seq data using regularized negative binomial regression. Genome Biol. 2019; 20:296. https://doi.org/10.1186/s13059-019-1874-1 PMID:31870423

7. Aran D, Looney AP, Liu L, Wu E, Fong V, Hsu A, Chak S, Naikawadi RP, Wolters PJ, Abate AR, Butte AJ, Bhattacharya M. Reference-based analysis of lung single-cell sequencing reveals a transitional profibrotic macrophage. Nat Immunol. 2019; 20:163–72. https://doi.org/10.1038/s41590-018-0276-y PMID:30643263

8. Ashburner M, Ball CA, Blake JA, Botstein D, Butler H, Cherry JM, Davis AP, Dolinski K, Dwight SS, Eppig JT, Harris MA, Hill DP, Issel-Tarver L, et al. Gene ontology: tool for the unification of biology. The Gene Ontology Consortium. Nat Genet. 2000; 25:25–9. https://doi.org/10.1038/75556 PMID:10802651

9. Gene Ontology Consortium. The Gene Ontology resource: enriching a GOld mine. Nucleic Acids Res. 2021; 49:D325–34. https://doi.org/10.1093/nar/gkaa1113 PMID:33290552

10. Mi H, Muruganujan A, Ebert D, Huang X, Thomas PD. PANTHER version 14: more genomes, a new PANTHER GO-slim and improvements in enrichment analysis tools. Nucleic Acids Res. 2019; 47:D419–26. https://doi.org/10.1093/nar/gky1038 PMID:30407594

11. Sergushichev A, Korotkevich G, Sukhov V, Artyomov MN. Fast gene set enrichment analysis. Biorxiv. 2019.

Supplementary Figures

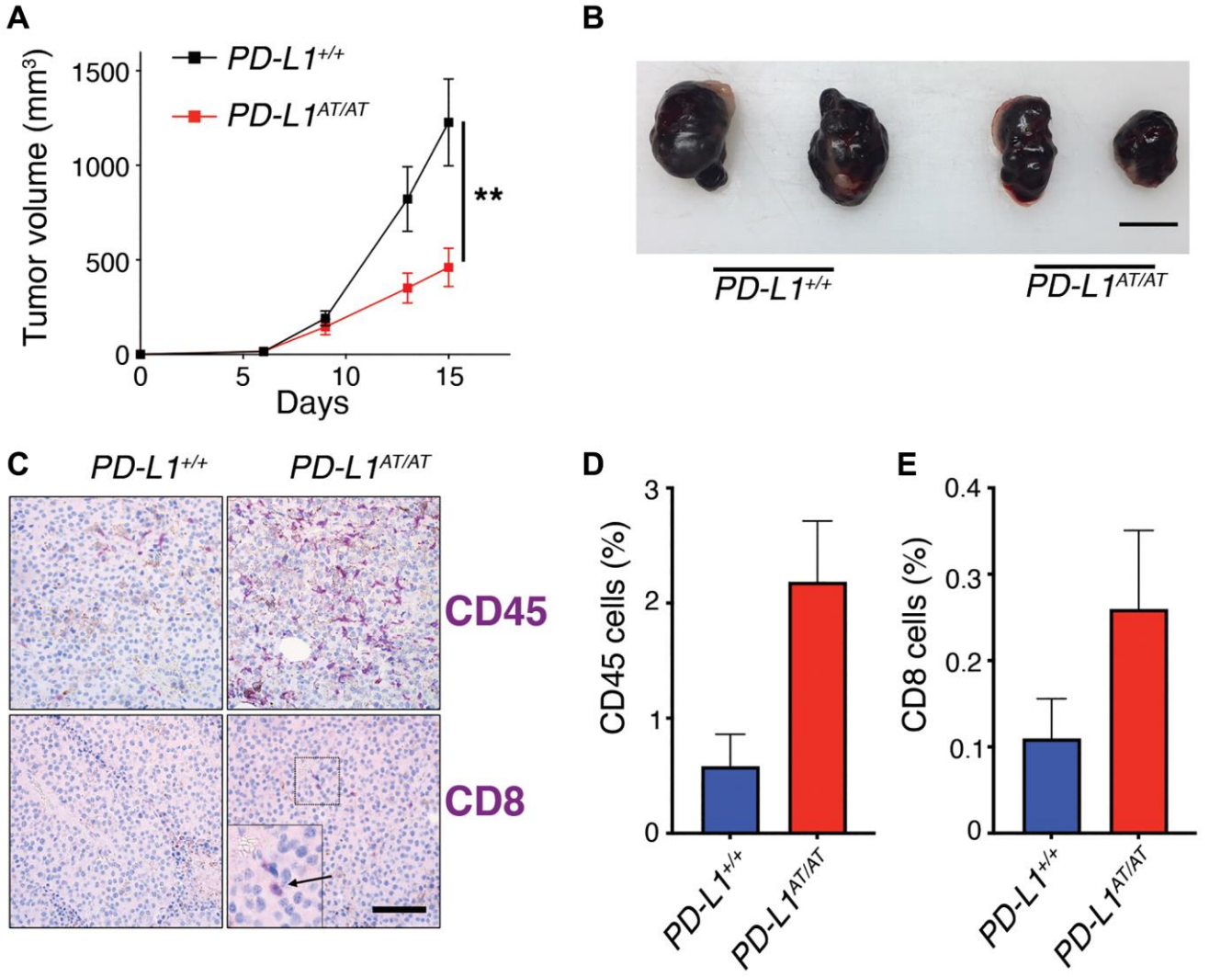

Supplementary Figure 1. Resistance to B16-F10 melanoma allografts in *PD-L1*$^{AT/AT}$ mice. (**A**) Growth of B16-F10 allografts subcutaneously implanted into the left flank of *PD-L1*$^{+/+}$ and *PD-L1*$^{AT/AT}$ mice. The *p* value was calculated with mixed-effects analysis. $^{**}p <$ 0.01 (**B**) Representative picture of the melanoma allografts from these analyses isolated at day 15. Scale bar (black) indicates 1 cm. (**C**) Immunohistochemistry of CD45 and CD8 in B16-F10 allografts isolated at day 15from of *PD-L1*$^{+/+}$ and *PD-L1*$^{AT/AT}$ mice. An inset is magnified to illustrate the presence of tumor-infiltrating CD8+ cytotoxic T cells in the allografts grown in mutant mice. Scale bar (black) indicates 100 µm. (**D**, **E**) Quantification of CD45+ (**D**) and CD8+ (**E**) cells from the analyses shown in (**C**).

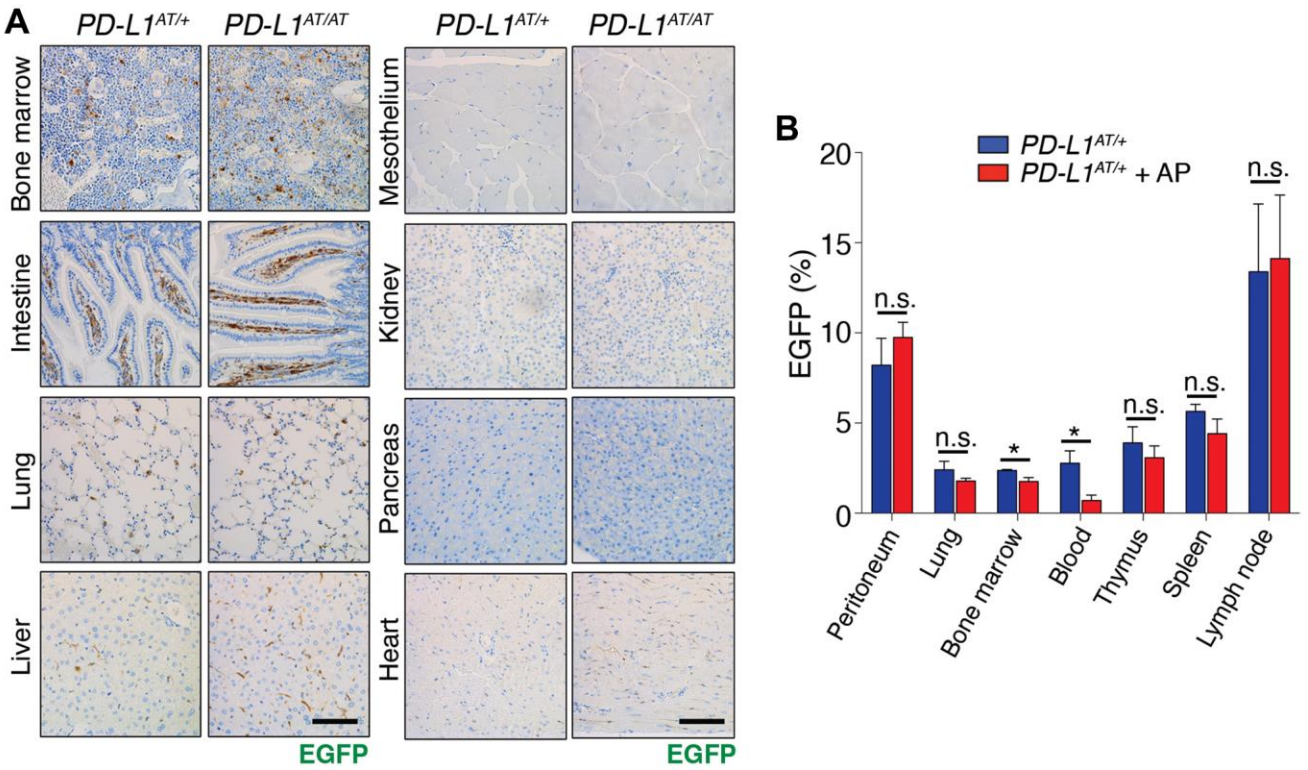

Supplementary Figure 2. Characterization of the PD-L1^{ATTAC} mouse model. (**A**) EGFP immunohistochemistry (IHC) from the bone marrow, intestine, lung, liver, mesothelium, kidney, pancreas and heart of *PD-L1*$^{AT/+}$ and *PD-L1*$^{AT/AT}$ mice. Scale bar (black) indicates 100 µm. (**B**) Percentage of EGFP+ cells as revealed by FACS in the indicated organs from control and AP-treated *PD-L1*$^{AT/+}$ mice. AP20187 (2.5 mg/kg) was administered via i.v. for three consecutive days. The *p* value was calculated with unpaired *t*-test. Abbreviation: n.s.: non-significant, $^{*}p < 0.05$.

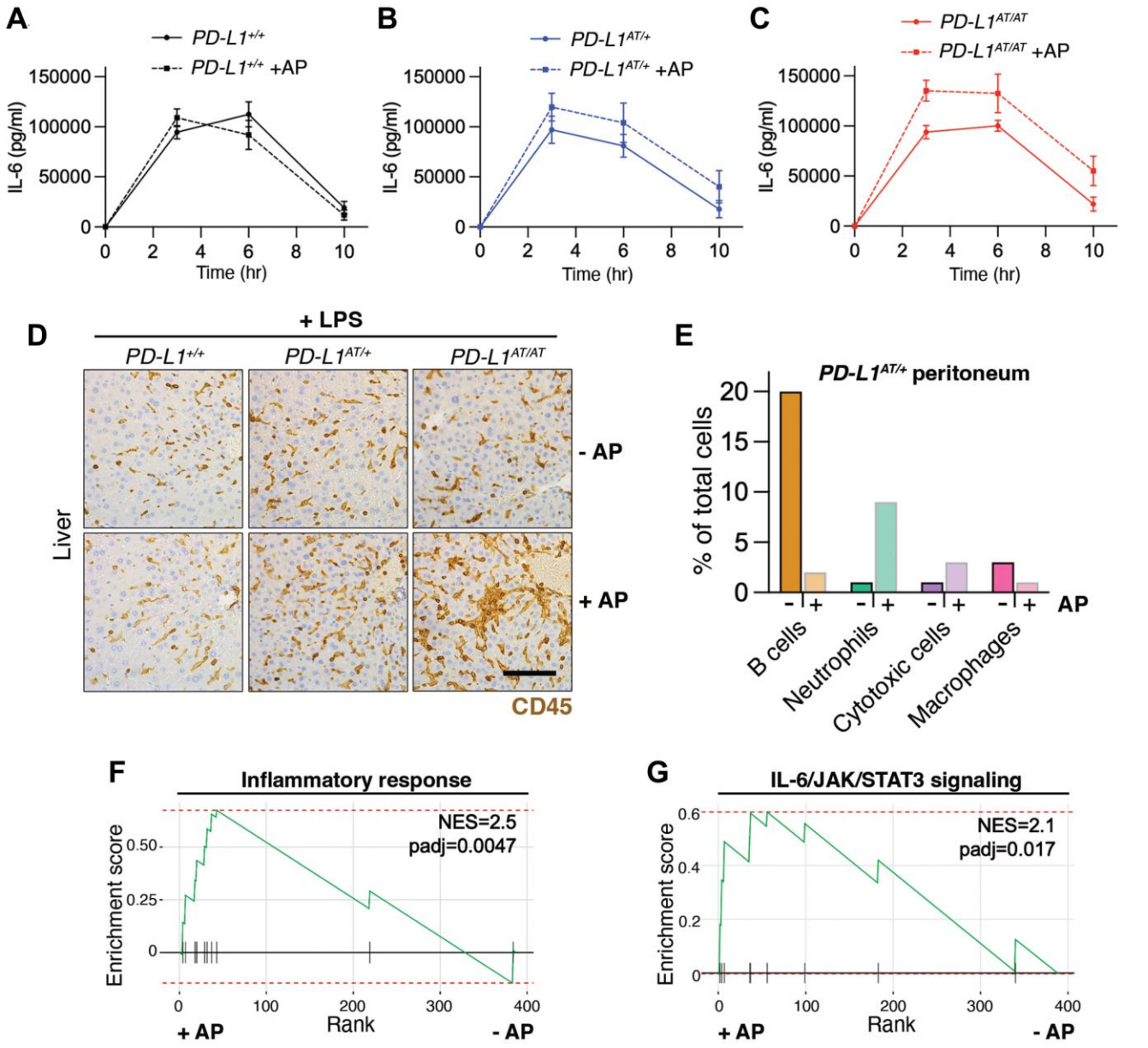

Supplementary Figure 3. Depletion of PD-L1^{+} cells sensitizes mice to LPS. (**A**–**C**) Kinetics of IL-6 accumulation and clearance in plasma isolated from *PD-L1*$^{+/+}$, *PD-L1*$^{AT/+}$ and *PD-L1*$^{AT/AT}$ mice after LPS injection as determined by ELISA. (**D**) IHC of CD45 in the livers of *PD-L1*$^{+/+}$, *PD-L1*$^{AT/+}$ and *PD-L1*$^{AT/AT}$ mice after LPS injection. Mice were treated via i.p. with AP (2.5 mg/kg) for 3 days and i.p. with 10 mg/kg LPS on the following day. Scale bar (black) indicates 100 μm. (**E**) Quantification from the single-cell sequencing analysis shown in Figure 4E, indicating the changes in the cell repertoire in the peritoneum from *PD-L1*$^{AT/+}$ mice upon AP treatment. (**F**, **G**) Preranked GSEA on the genes from the hallmarks "Inflammatory response" (**F**) and "IL-6/JAK/STAT3 signaling" (**G**) obtained from scRNAseq data comparing the transcriptomes of cytotoxic cells from *PD-L1*$^{AT/+}$ mice upon AP treatment.

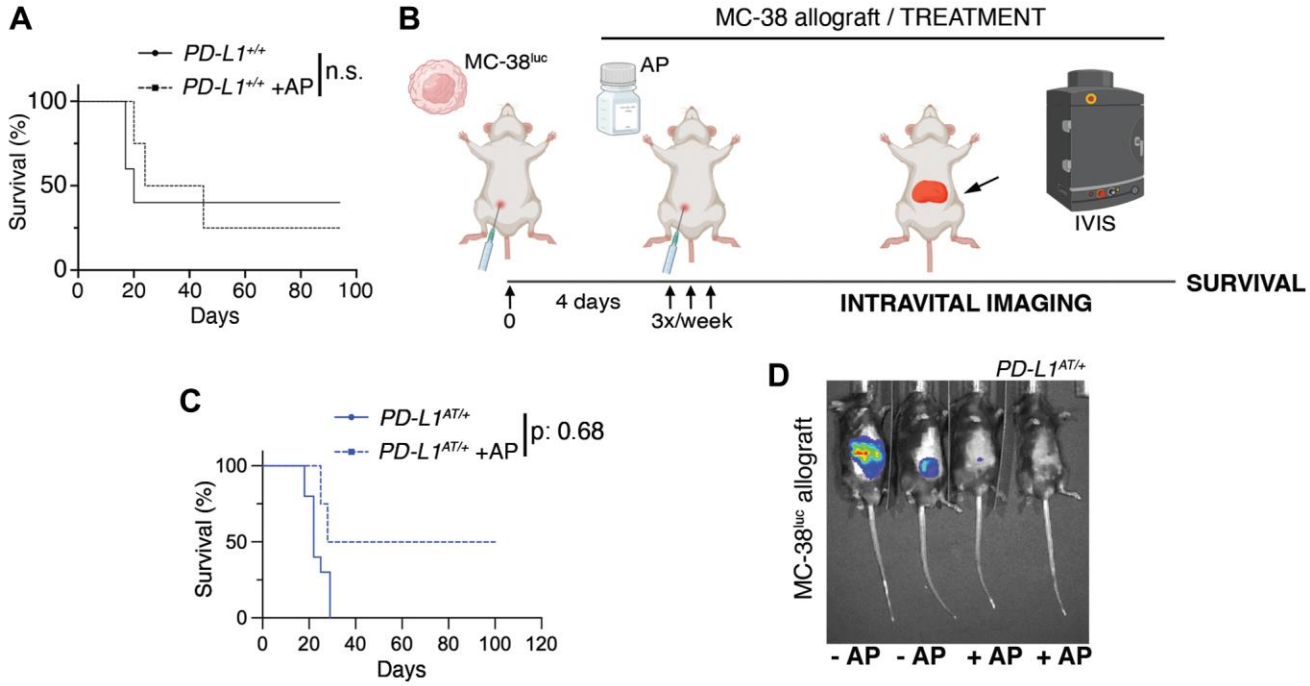

Supplementary Figure 4. Impact of depleting PD-L1^{+} cells in MC-38^{luc} allografts. (**A**) Kaplan-Meier survival curve of control and AP20187-pretreated *PD-L1*$^{+/+}$ mice after i.p. inoculation of MC-38^{luc} allografts. The *p* value was calculated with the Mantel-Coxlog rank test. Abbreviation: n.s.: non-significant. (**B**) Schematic overview of the treatment experimental workflow. 5 × 10^{5} MC-38^{luc} cells were intraperitoneally injected into mice. 4 days later mice were injected i.p. with AP20187 (2.5 mg/kg) 3 times a week for the duration of the experiment. (**C**) Kaplan-Meier survival curve of control and AP20187-pretreated *PD-L1*$^{AT/+}$ mice after i.p. inoculation of MC-38^{luc}allografts in the treatment model. The *p* value was calculated with the Mantel-Coxlog rank test. (**D**) Representative IVIS image of mice from the experiment definedin (**C**).